SELECTIVE GROWTH OF THERMO-RESPONSIVE POLYMER BRUSHES THROUGH ORTHOGONAL SELF-ASSEMBLY

by

ABUL BASHAR MOHAMMAD GIASUDDIN

(Under the Direction of Jason Locklin)

ABSTRACT

In this work, thermally responsive poly(N-isopropyl acrylamide) or p(NIPAM) brushes were successfully grafted to multi-component surfaces with chemical selectivity. A catechol based photo-initiator was synthesized and selectively assembled on the surface prior to polymerization. Orthogonal formation of both monolayers and surface selective polymer brushes were confirmed by FTIR. Thick and homogeneous growth of pNIPAM polymer brushes selectively on TiO_2 surfaces with dual SiO_2-TiO_2, was observed using SEM and optical microscopy. Controlled growth of pNIPAM brushes was possible using both different monomer concentrations and photo-irradiation time. Thickest brushes were achieved at saturation concentration of monomer (87% w/w) in solvent and a linear growth in polymer brush thickness formation was observed up to 20 hours of irradiation. The thermal responsive behavior of pNIPAM brushes was confirmed using static contact angle below and above the LCST (Lower Critical Solution Temperature) of pNIPAM. Swelling studies were also performed to estimate the water uptake and release from brush layers below and above LCST.

INDEX WORDS: polymer brushes; pNIPAM; orthogonal self-assembly

SELECTIVE GROWTH OF THERMO-RESPONSIVE POLYMER BRUSHES THROUGH ORTHOGONAL SELF-ASSEMBLY

by

ABUL BASHAR MOHAMMAD GIASUDDIN

B.Sc., BANGLADESH UNIVERSITY OF ENGINEERING AND TECHNOLOGY, BANGLADESH, 2003

M.S., GWANGJU INSTITUTE OF SCIENCE AND TECHNOLGY, REPUBLIC OF KOREA, 2006

A Thesis Submitted to the Graduate Faculty of The University of Georgia in Partial Fulfillment of the Requirements for the Degree

MASTER OF SCIENCE

ATHENS, GEORGIA

2011

SELECTIVE GROWTH OF THERMO-RESPONSIVE POLYMER BRUSHES

THROUGH ORTHOGONAL SELF-ASSEMBLY

by

ABUL BASHAR MOHAMMAD GIASUDDIN

Major Professor: Jason Locklin

Committee: Leidong Mao
Zhengwei Pan
William Kisaalita

Electronic Version Approved:

Maureen Grasso
Dean of the Graduate School
The University of Georgia
August 2011

DEDICATION

I would like to dedicate this thesis work to my mother

ACKNOWLEDGEMENTS

I am very grateful to my advisor Dr. Jason Locklin, for mentoring me in my graduate study and research. I could not have written this thesis without his guidance and direction. He has continuously helped me learn how to work harder and to progress since my first days at his lab.

I like to thank my thesis committee members: Dr. Leidong Mao, Dr. Zhengwei Pan and Dr. William Kisaalita for their advice. I am very grateful to an amazing group of fellow graduate students in the Locklin Lab: Kristen Fries, Sara Orski, Kyle Sontag, Gareth Sheppard, Vikram Dhende, Joe Grubbs, Rachelle Arnold, Evan White, Jenna Bilbrey and our former post-doc Dr. Satya Samanta.

TABLE OF CONTENTS

Page

LIST OF TABLES

Page

LIST OF FIGURES

Page

CHAPTER 1

BACKGROUND AND LITERATURE REVIEW

Polymer brush definition

Polymer brushes first gained attention in the scientific community in the 1950s, after the discovery that flocculation could be prevented by grafting polymer molecules to colloidal particles (1). In the early 1990s, several groups performed detailed studies on polymer brushes and helped to create an increased awareness of these types of structures (2). Since then, polymer brushes have become an area of great attention. Polymer brushes can be defined as an array of macromolecular chain ends that are covalently tethered to a surface with a density high enough to alter the unperturbed solution dimensions of the chains (3).

The quantitative characterization of a polymer brush can be expressed as the reduced tethered density ($\sum$); $\sum = \sigma\pi R_g^2$, where R_g is radius of gyration of a tethered chain at specific experimental conditions of solvent and temperature and σ is the grafting density. Grafting density is determined by $\sigma = \rho h N_A/M_n$; where h is brush thickness; ρ, bulk density of the polymer brush composition; N_A is Avogadro's number; and M_n is the number average molecular weight (1).

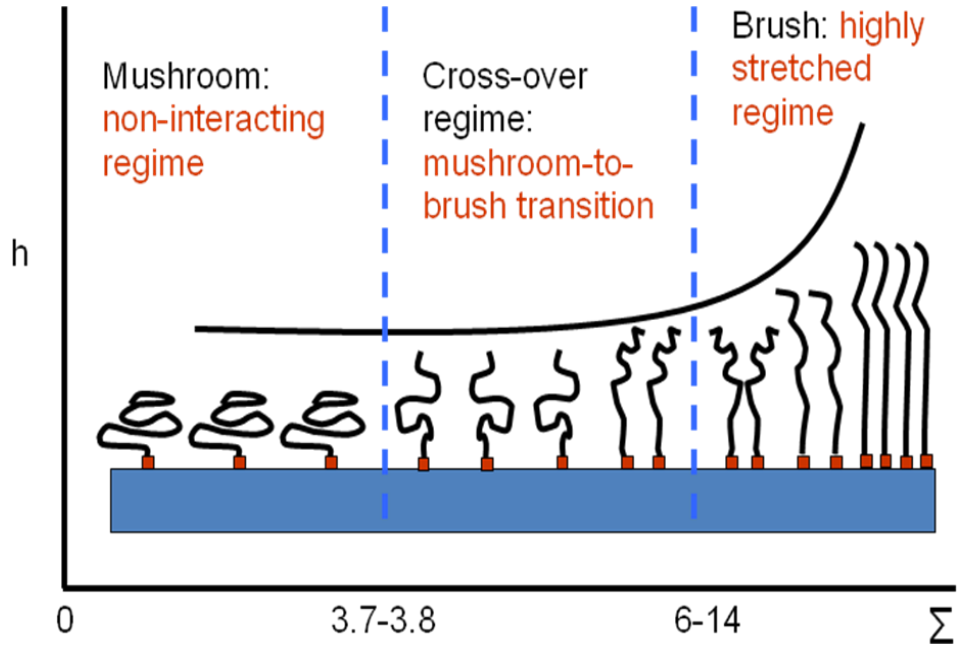

Figure 1. Depiction of mushroom, crossover, and brush regimes of grafted polymer thin films in relation to brush thickness (h) and reduced tethering density (Σ).

Reduced tethered density (∑) is physically interpreted as the number of chains that occupy an area that a free nonoverlapping polymer chain would normally fill under the same experimental conditions (1). Brush-like character of the grafted film is categorized on the basis of this value (Figure 1).

It is generally recognized that three regimes occur in brush formation:

(1) The ‘‘mushroom’’ or noninteracting regime ($\sum < 3.8$),

(2) The crossover regime or mushroom-to-brush transition regime ($3.8 < \sum < 6$), and

(3) The highly stretched regime ($\sum > 6$).

The transition between single grafted chains and a polymer brush is loosely defined because of the statistical characteristic of grafting and polydispersity of the tethered chains. Resulting fluctuations of the average distance between grafting points can cause an inhomogeneous distribution of across the grafting surface (1).

Synthesis of polymer brushes

Synthesis of polymer brushes can be categorized into two groups based on the chemical interaction between polymer and substrate:

1. Physical Sorption and
2. Chemical Sorption.

Physical Sorption

Physical Sorption (or Physisorption) is the physically adsorption of polymeric chains on solid surfaces (4-6). Block copolymers provide a general example. In this method, the surface and solvent can be chosen to maximize preferential adsorption of one block to a solid surface while the solvent is chosen to preferentially interact with the other block of a diblock polymer. For example, physisorption of polystyrene-b-

poly(ethylene oxide) (PS-b- PEO) from a toluene solution where the PEO segment is attracted to a mica surface while the PS block is preferentially solvated. More examples of polymer adsorption with only physical interactions are obtained through techniques such as spin coating, spraying, painting etc. Physisorption displays several disadvantages, it is unstable under certain conditions of solvent and temperature, and/or can be displaced by other adsorbents. Figure 2 illustrates the physisorption of polymer on the substrate.

Figure 2. Schematic illustrations of polymer brush growth in a physical sorption method.

Chemical Sorption

Chemical Sorption (or Chemisorption) is the covalent attachment of polymer chains at the interface. Due to covalent bond between polymer and substarte, this method enhances the stability of the tethered polymer layers. Covalently attached polymer chains can be synthesized by either the ‘‘grafting-to’’ or ‘‘grafting-from’’ methods.

The scheme in Figure 3 shows both type of chemisorptions “Grafting to” (Figure 3a) and “ Grafting from” (Figure 3b).

Grafting To:

The “grafting to” approach is similar to spontaneous adsorption of self-assembled monolayers. In this method a preformed polymer with a reactive end-group is used as the precursor, and the reaction typically occur in liquid phase in order to attach the polymer onto substrates (7). Some of the common reactive functional groups are thiols, silanes, carboxylic acids, and phosphonic acid. One disadvantage of the “grafting to” approach is that it is often difficult to react the end group of a high molecular weight polymer chain with a surface with high yield, the thermodynamics and kinetics of the process also restrict the grafting density. Also, due to chemical compatibility requirements, the available systems with suitable reactive end groups and compatible functional units in the polymer chain are limited in scope.

a)

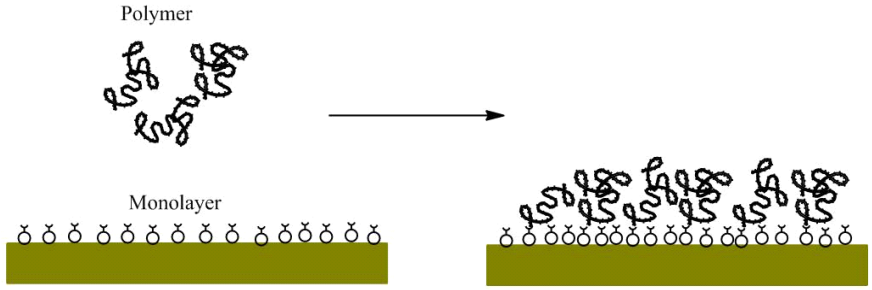

b)

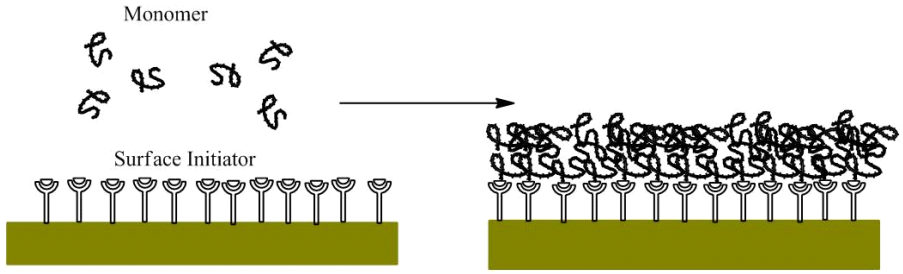

Figure 3. Schematic illustration of polymer brushes by Chemisorption polymerization, a) "Grafting to" and b) "Grafting from" method.

Grafting from:

In the "grafting form" approach, polymer chains are synthesized from a surface through immobilization of a monolayer of surface-initiators followed by in-situ polymerization of selected monomers. This approach is often referred to as surface-initiated polymerization (SIP). The "grafting from" method is significantly more versatile than "grafting to", and it has been shown that, through SIP, it is possible to assemble densely packed polymer brushes with low polydispersities from a large variety of

monomers in a controllable fashion (8). If there is no free initiator in solution, polymerization occurs exclusively at the surface. Importantly, the grafting density of the polymer chains can be finely tuned by varying the grafting density of the surface initiator (9-10). Because of its versatility, reliability, and control, "grafting from" is attracting significant scientific interest, and is being utilized in application areas such as colloid stabilization, new adhesive materials, protein-resistant bio-mimetic surfaces, chromatographic separation of organic and biomaterials, and organic-inorganic nanocomposites (11-13).

Almost all available polymerization techniques have been applied to graft polymers from substrates. These includes, conventional free radical polymerization, ring opening polymerization, anionic polymerization, cationic polymerization, ring opening methathesis polymerization (ROMP), nitroxide mediated polymerization, atom transfer radical polymerization (ATRP), reversible addition fragmentation chain transfer (RAFT) polymerization (12). One thing that has not been thoroughly investigated is pattering and increased complexity of different chemical functionality spatially distributed in a controlled fashion. Surface-initiated photopolymerization can be an effective and convenient technique to overcome this problem (14-17). Free-radical polymerizaiton by photochemical initiation has distinct advantages, such as ability to build thick brushes, homogeneous distribution of polymer brushes, tolerance for moisture, wide application to a variety of organic functional groups, low cost of operation and potentially reducing negative effects on the bulk polymer (18).

Applications of Polymer Brushes

Polymeric chains as brushes exhibit many distinctive properties compared to polymeric chains in solution. Based on those distinctive properties polymer brushes can be used for multi-dimensional applications. Some of the applications of polymer brushes are highlighted below:

Stabilization

Colloidal stability against agglomeration is important in many industrial processes. Stabilization or compatibilization is normally carried out by encapsulating a colloid or particle within a shell of organic polymer; which results in a property mismatch between the composite layers (12). The surface properties of the shell aid or create the desired stabilization. We can get improved properties by compatibilization of colloid or core-shell particles with polymer brushes, as has been demonstrated in the stabilization of latex polymers coated with polymer brush layers (19).

Surface coatings

One of the most important fundamental characteristics of surface properties or surface interfaces is adhesion. Surfaces can be functionalized with proteins and cells by physisorption and "grafting to" polymerization methods (20, 21). For example, tissue compatibility has been engineered by creating poly(acrylic acid) polymer brushes on the poly(vinylidene difluoride) surfaces through conversion of the acid-functionalized brush to a fibronectin-coated surface using carbodiimide coupling (22). Polymer brush-coated surfaces also have the ability to provide nonfouling properties. Extracellular proteins strongly adsorb on many surfaces through hydrophobic interactions. Sometimes it is

problematic when specific surface interactions are to be studied, as the co-adsorbing proteins interfere with the desired surface chemistry (23-26).

Super hydrophobic surfaces have been created using patterned polymer brushes and grafted polymer brushes have been used to control wetting (27). By functionalizing a surface with polymer brushes, the morphology can influence the overall performance. The morphology of ultrathin poly-(styrene-b-butadiene-b-styrene) copolymer films deposited on polystyrene brushes has been found to be influenced by grafting density and the DP (degree of polymerization) of the underlying polymer brush layer (28).

Polymer coatings prepared electrochemically tend to have highly desirable properties such as good adhesion and they can be formed on virtually any shaped substrate. However, this process is limited by the final coating thickness, as the electropolymerization is self-limiting and thin brushes are mechanically fragile. Thicker coatings can be produced by sequentially coupling cathodic electropolymerization with another polymerization method. In this way, polymer brushes can be produced on electrically conductive using acrylate-substituted monomers that are functionalized to undergo ATRP and ROMP "grafting from" methodologies (12).

Separations

Polymer brushes have been used in chromatographic protein separation and purification (29). Depending on specific solute, solvent, and polymer brush interactions, the quality of separation depends on surface density and chain length of the surface-attached polymer chains, solvent size, and polarity (30). The attachment of polymer brushes to membranes can impact a variety of fluid flow properties. Appropriately functionalized membrane surfaces can improve or enhance separation and resolution through selective adsorption of one component in a mixture (12).

Polymer brushes have also been used as microvalves for the control fluid flow (31). Theoretical investigation of the flow of a good solvent through two closely spaced polymer brush-coated surfaces revealed that the brushes respond to the flow by expanding in response to a shear flow, which causes a decrease in the cross-sectional flow area and a reduction in the flux rate. This pressure-sensitive behavior allows the polymer brush to act as both a sensor and a self-regulating valve. Modeling this behavior revealed that several flow regimes exist and these were found to be dependent on brush height and gap distance between closely spaced parallel plates. It has been found that more sensitive microvalves would result with loosely grafted brushes than with densely grafted brushes (32). Polymer brushes also can be used to create channels which can be opened and closed by controlling solvent properties and pH (33).

Nanofabrication

A combination of “top down” and “bottom up” approaches can be used to pattern and prepare polymer brushes with controlled composition and size of nanoscale features. Researchers at IBM used contact-molding to transfer the pattern from an electron beam-fabricated silicon wafer master to a photopolymer matrix, which contained inimers as one component of the formulation (34). Once casted, the surface-exposed inimers were used as sites for “grafting from” ATRP and nitroxide living free radical polymerization chemistries to produce well controlled polymer brushes with styrene, methyl methacrylate, and hydroxyethyl methacrylate. Through this process, less than 60 could be replicated, with thicknesses ranging from 10 to 143 nm on both flat and nanopatterned surfaces (35).

Surfaces for Electronics

Polymer brushes have been used to make both insulating and conducting surfaces. One of the applications of polymer bruses is as a template in the fabrication of conducting polymer and complementary gold microstructures. Patterned structures can be achieved by acting as the insulating layer during electrodeposition (36). A number of semiconductor processing issues can be improved, by directly attaching polymer brushes to silicon surfaces (37). Conductive polymers can be grafted onto polyethylene and poly(styrenesulfonic acid) films to give conductive poly(thiophene) and poly(ethylenedioxythiophene) surfaces. Chemical sensors based on semiconductive poly(p-phenylene ethynylene) brushes have shown improved stability and displayed

higher emission quantum yields relative to spin-cast films because of reduced aggregation of these systems (38-39).

Stimuli-responsive polymer brushes

Polymeric brushes that are responsive to external stimulation are called stimuli-responsive polymer brushes. This kind of coating shows great promise for direct application in areas like sensor systems, drug delivery, microfluidic devices and membrane technology (40-43). The use of external stimuli (e.g., temperature, pH) to effect a change in polymer properties has also been found to be very useful for controlling adhesion on biosurfaces. Among all the stimuli-responsive brushes, particularly thermo-responsive brushes, poly (N-isopropylacrylamide) (pNIPAM) has attracted great attention due to its specific characteristics at Lower Critical Solution Temperature (LCST).

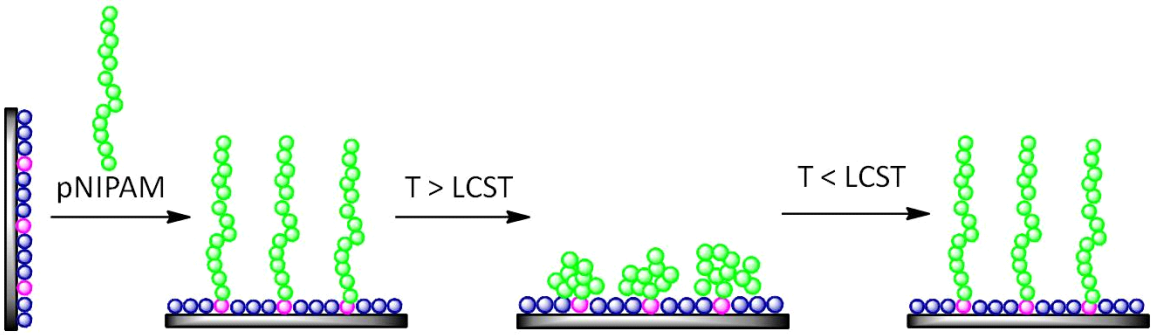

Figure 4. Schematic illustration of pNIPAM polymer brush behavior below and above the LCST of pNIPAM

pNIPAM undergoes a phase change when taken through its LCST, observed at 32°C. The LCST can be manipulated by changing the N-substituted hydrocarbon chain or through the preparation of copolymers (44).

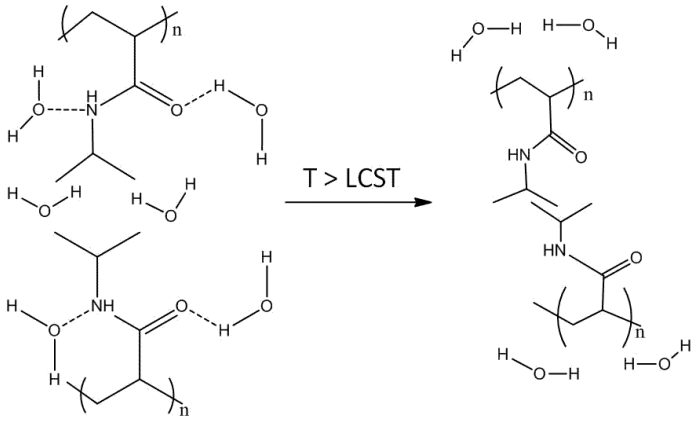

Figure 5. Water dissociation process of pNIPAm structures at temperatures above the LCST of pNIPAM.

At the LCST, reversible dehydration of the hydrocarbon side chain occurs, causing a collapsed conformation and a change from a hydrophilic to a hydrophobic state, which can result in solubility changes for bulk polymers in solution. This allows for switching of drug reservoirs, microfluidic valves and membrane pores (45-51). Since pNIPAM expels its liquid contents at a temperature near that of the human body, pNIPAM has been investigated by researchers for possible applications in controlled drug

delivery (52). A particular advantage of such polymer based devices is their simple design, which provides the basis for cost-effective fabrication and miniaturization (53).

Orthogonal assembly of molecule

The concept of orthogonal self-assembly was first introduced by Laibinis and Whitesides (54). They reported the selective adsorption of two different adsorbates from a common solution onto a substrate exposing two different materials at its surface. Later orthogonal assembly has also been demonstrated in the presence of two metals (ex. Au and Pt) using isonitriles and thiols (55, 56). The most significant advantage of spontaneous self-assembly over conventional photolithography is in the surface patterning process. In conventional photolithography, different chemical functionality can be incorporated onto a flat substrate routinely using the combination of several patterning and surface activation steps. But in case of three-dimensional and irregularly shaped objects, or when feature size gets smaller and smaller, this technique is not applicable.

Orthogonal functionalization on oxides surfaces can be achieved through either selective deprotonation of a photabile end group or through the oxidation of a homogenous monolayer (57). Selective functionalization on oxides is often found to be difficults with certain anchor groups such as tricholosilanes due to high reactivity, which oligomerize upon exposure to water and can physisorb to almost any surface (58). So selecting specific anchor group on certain oxide surface is currently a major challenge for orthogonal functionalization.

Catechols, are known to chelate a variety of metal oxides via a mononuclear bidentate coordination (59-64). It's self-assembly on TiO_2 and Al_2O_3 has been exploited in creating both protein resistant surfaces and attaching organic semiconductors to dielectric surfaces (65-67). In our initial studies we have observed that this bidentate coordination cannot occur on SiO_2 which means no appreciable monolayers were formed under acid, base, or neutral conditions at room temperature. This characteristic of catechols make it avery suitable anchor group for orthogonal functionalization in TiO_2-SiO_2 or SiO_2-Al_2O_3 surfaces.

CHAPTER 2

THESIS OBJECTIVE

The research objective of this thesis is to selectively grow thermo-responsive polymer brushes on multi-component surfaces through orthogonal self–assembly. To achieve this, our first aim is to synthesize initiator which can orthogonally form monolayers on multi component surfaces. Once the initiator has been synthesized with surface selectivity, we aim to grow thermo-responsive polymer brushes based on pNIPAM using free-radical polymerization through photo-initiation. We will then investigate the growth of pNIPAM brushes by controlling the monomer concentration and polymerization time. After the growth of pNIPAM brushes, we will perform experiments to characterize the pNIPAM brushes and will analyze some of the basic thermo-responsive behavior of grown polymer brushes in both *in-situ* and *ex-situ* above and below LCST.

CHAPTER 3

EXPERIMENTAL DETAILS

Materials

Silicon wafers (orientation ⟨100⟩, native oxide) were purchased from University Wafer. Tetrahydrofuran (THF), purchased from BDH, was distilled from sodium-ketyl. N-isopropylacrylamide (NIPAM) was purchased from TCI and flashed through a basic alumina column to remove inhibitor prior to polymerization. Methanol and dichloromethane (DCM) were purchased from BDH. Dichloromethane (DCM) was distilled over calcium hydride and degassed using freeze-pump-thaw methods. Solvent anhydrous dimethylformamide (DMF) (Drisolv, 99.8%by GC) were purchased from EMD. All other chemicals were purchased from Sigma Aldrich and were used as received.

Synthesis of Photo-initiator

4,4′-Azobis(4-cyanovaleric acid) (2.19 g, 7.8 mmol) was added to thionyl chloride (50 mL) under nitrogen atmosphere. The reaction mixture was refluxed for 15 min in a 100 °C oil bath.

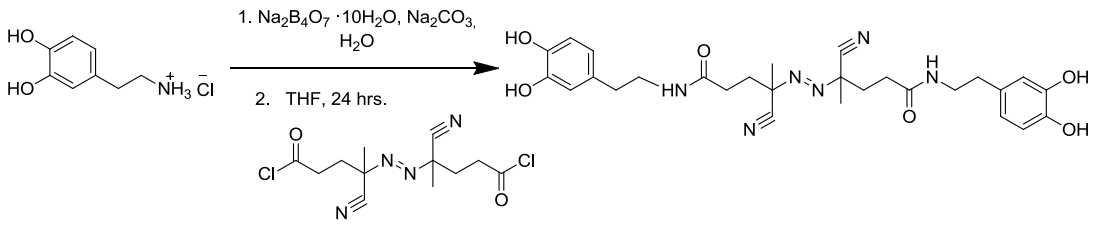

Figure 6. Synthesis of 4,4'-(diazene-1,2-diyl)bis(4-cyano-N-(3,4-dihydroxyphenethyl)pentanamide) (AIBN-catechol)

The hot solution was immersed in an ice bath and cooled to room temperature. Excess thionyl chloride was removed by vacuum evaporation at room temperature to yield a yellow solid. To the crude product was added 25 mL of dry tetrahydrofuran and the solution was bubbled with argon gas one hour to remove dissolved oxygen. In a separate flask, sodium borate decahydrate (2.97 g, 7.8 mmol) was dissolved in 18 MΩ nanopure water (40mL) and also deoxygenated with argon gas for one hour. Dopamine HCl (2.975 g, 15.7 mmol) was added to the water solution, followed by sodium carbonate (2.66 g, 25.11 mmol) and dissolved. The aqueous solution was kept under inert atmosphere and chilled to 0 °C in an ice bath and stirred vigourously. The THF/cyanovaleric acid chloride solution was added dropwise to the chilled solution and

stirred 24 hours. The reaction mixture was acidified to pH 2 using 2M HCl solution and washed three times with 30 mL portions of ethyl acetate. The ethyl acetate layers were collected, dried with $MgSO_4$, and evaporated to dryness. The crude product was purified by column chromatography using ethyl acetate/hexane (2:1) as the eluent. The product was a yellow solid. 0.923g, 25.6% yield. ^{1}H NMR (DMSO D_6, 300 MHz) δ (ppm): 8.02 (br s, 1H, OH); 8.00 (br s, 1H, O*H*); 6.61 (d, 7.9 Hz, 2H, Arom.); 6.57 (s, 2H, Arom.); 6.44 (d, 8.0 Hz, 2H, Arom.); 6.34 (br s, 1H, N*H*); 3.18 (d, 5.9 Hz, 4H, CH_2NH); 2.54 (d, 7.6 Hz, 4H, CH_2CH$_2$NH); 2.38-2.24 (m, 8H, CH_2); 1.68 (s, 3H, CH_3); 1.64 (s, 3H CH_3). ^{13}C NMR (DMSO D_6, 300 MHz) δ (ppm): 173.29, 145.70, 144.16, 130.81, 119.84, 116.58, 116.11, 72.62, 35.23, 33.94, 32.69, 30.71, 23.60, 21.42.

TiO_2 Deposition

Stripes of 1 cm wide TiO_2 were deposited onto clean silicon wafers (University Wafer) by physical vapor deposition from a TiO_2 target using magnetron sputtering (PVD75, Kurt J. Lesker). A tape mask was used to control stripe width. Wafers were rinsed with isopropanol and dried before deposition. The TiO_2 was deposited at 0.5 Å/s using a 50 W power setting and a 5 mTorr capman pressure.

Orthogonal Self-Assembled Monolayer Formation

TiO_2 deposited silicon wafer were cut into 1 cm by 2 cm pieces with equivalent amounts of exposed TiO_2 and SiO_2. Then all pieces were rinsed with methanol and N_2 dried. Substrates were Ar plasma cleaned (Harrick Plasma, PDC-32G) on high (18W) for 5 min. The cleaned wafers were placed in methanol with 1 mg/ml catechol photo-initiator

(Scheme 1) and in the dark for 12 hr. The catechol monolayers were rinsed with methanol. Formation of the TiO_2 selective monolayer was confirmed by ellipsometry.

Photoinitiated Polymerization

NIPAM was dissolved in degassed DCM in a glove box under nitrogen atmosphere. Substrates and dissolved NIPAM were placed in a glass vial and sealed. Vials were placed in a UV light (350 nm) reactor (Rayonet, RPR-600) overnight. NIPAM polymer was grown from the surface and in solution. In order to remove physisorbed polymer, the contents of the vial were soxlet extracted in THF for 12 hrs. Polymer brushes were rinsed with THF and N_2 dried.

Characterization Methods

Fourier transform-infrared (FT-IR) measurements were taken with a Nicolet model 6700 instrument with a grazing angle attenuated total reflectance accessory (GATR, Harrick Scientific) at 264 scans with 4 cm^{-1} resolution. The film thickness was measured using null ellipsometry performed on a Multiskop (Optrel GbR) with a 632.8 nm He-Ne laser beam as the light source at 70° angle of incidence. Both, Δ and Ψ, were measured and thickness was calculated by integrated specialized software. Several brushes were thicker than the limit allowed by null ellipsometry due to the asymptotic Ψ function. Brushes above this limited were characterized by profilometry using a Dektak 150 stylus profiler. Measurements were taken at 0.1 μm/sample using a 0.2 μm tip with a stylus force of 3.00 mg. At least three measurements were taken for each brush, and the

average thickness was recorded. Where applicable, brush thickness was confirmed by null ellipsometry and profilometry.

Spectroscopic ellipsometry (M-2000V, J.A. Woollam Co., Inc.) was used to track the dynamics of swelling. *Ex situ* measurements were taken at 65°, 70°, and 75° in order to fit the refractive indices and film thicknesses of the dry pNIPAM brush using specialized software provided by the company. Substrates were characterized after each film addition, reducing the number of variables required to fit the model over the spectral range, 380-1000 nm. *In situ* measurements were performed in a flow cell at a 60° angle of incidence. The Δ and Ψ values were monitored as the temperature of the water within the cell was cycled between 25 °C and 50 °C.

Contact angles of water drops were measured (Kruss, DSA100) using a white light source and a CCD camera. The syringe is fixed in an automatic dispenser that controls the size and deposition of the droplet. The contour of a sessile drop is analyzed and fitted to the Young-Laplace equation using a contour tracing algorithm that distinguishes the drop from the surface. For statistical purposes, at least three drops were measured on each sample. The reported contact angles are the average of these measurements.

Scanning electron microscopy-energy dispersive spectroscopy (SEM-EDS) (FEI Inspect F FEG-SEM equipped with EDAX EDS) was used to image the orthogonal nature of the self assembly. SEM was controlled by xTm (ver. 4.1.0.1910). The sample

was placed on the sample holder with double sided adhesive conductive carbon tape and was ready for analysis. The sample was set on its side to image the polymer brush from the side.

CHAPTER 4

RESULT AND DISCUSSION

In our study, we first synthesized AIBN-catechol photo-initiator specifically selected for orthogonal monolayer formation on TiO_2. Then orthogonal self-assembled monolayers (SAMs) were then formed on the TiO_2 part of SiO_2-TiO_2 dual surfaces using the catechol based initiator. Once the SAMs were formed on selective parts of the substances, pNIPAM brushes were grown using photo-initiated free radical polymerization. A schematic Illustration of the total process can be seen Figure 7.

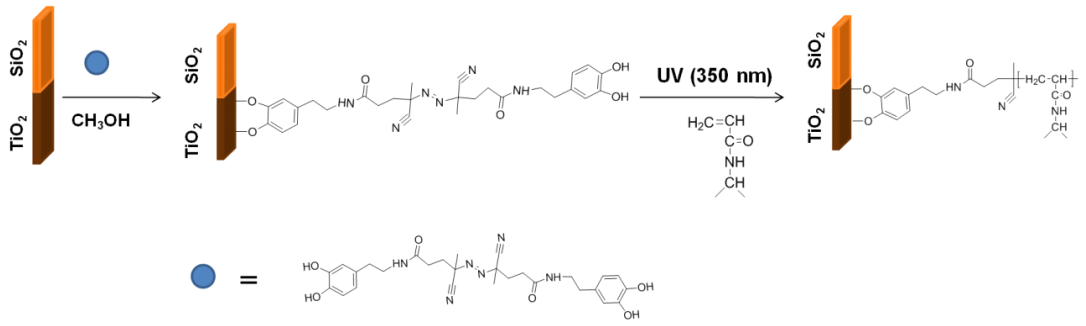

Figure 7. Schematic of orthogonal monolayer and polymer brush formation on SiO_2 - TiO_2 dual surfaces.

Orthogonal Self Assembled Monolayers (SAMs) were formed using 1 mg/ml AIBN-catechol based initiator (the structure of which is shown on figure 7) in methanol solution overnight, which generated a 2 nm homogeneous SAM selectively on TiO_2. Ellipsometric data confirmed the absence of monolayer on the SiO_2. Thermo-responsive pNIPAM polymer brushes were grown from TiO_2 surface by photo-irradiating SAMs of AIBN-catechol photo-initiator in an O_2 free environment. In presence of UV (350nm) the AIBN-catechol generates radicals, which initiates the growth pNIPAM brushes.

Surface Characterization of pNIPAM Polymer Brushes

FTIR spectra of orthogonal self-assembled monolayer and pNIPAM brush on TiO_2 surfaces are demonstrated in Figure 8a and Figure 8b.

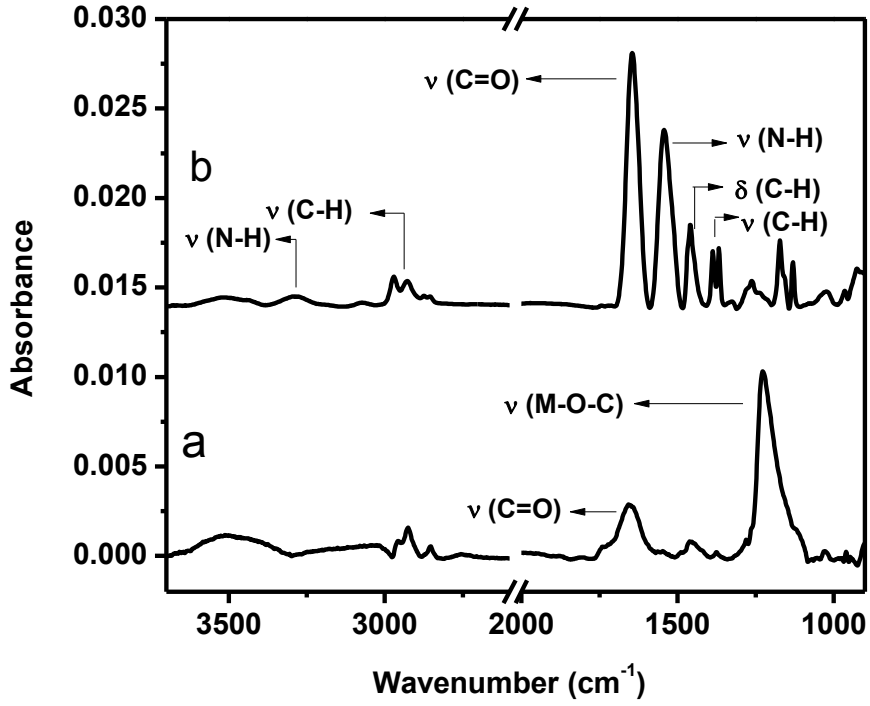

Figure 8. FTIR spectra of (a) AIBN-Catechol monolayer and (b) pNIPAM brush on TiO_2 surfaces.

Deprotonated, metal co-ordinated stretching of C-O group at 1235 cm^{-1} in Figure 8a confirmed the catechol monolayer formation on TiO_2 (60). In Figure 8b, the absorption peak at 3285 cm^{-1} and 1540 cm^{-1} indicate the stretching of the secondary amide group. Peak at 2960 cm^{-1} is due to asymmetric stretching of $-CH_3$ group and 1460 cm^{-1} is due to asymmetric bending of $-CH_3$ group. Strong absorption peak at 1650 cm^{-1} is

due to secondary amide C-O stretching. Stretch for two $-CH_3$ groups of the isopropyl functionality can be seen peak at 1369 cm^{-1} and 1389 cm^{-1}. Observed bending and stretches confirmed the formation of covalent bond of pNIPAM brush (68, 69).

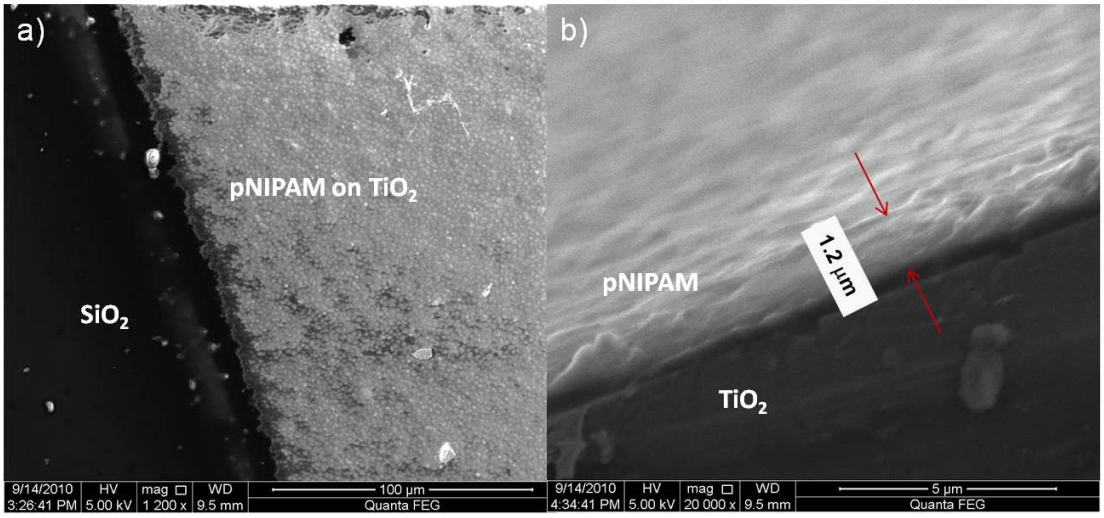

Figure 9. SEM images of selective growth of pNIPAM brush on TiO_2 of SiO_2-TiO_2 surfaces. Polymerization time was 24 hours and saturated concentration of NIPAM (87% (w/w)) monomer was used. a) Top view of pNIPAM brush, and b) Cross sectional view of pNIPAM brush.

Figure 9 shows a representative SEM image of the dual surface with the selective growth of pNIPAM from the TiO_2 surface. Figure 9a clearly shows the NIPAM polymer brush growth on TiO_2 with no coating observed on SiO_2, which confirm the

homogeneous orthogonal growth of pNIPAM from catechol based intitiator. Figure 9b shows the cross sectional view of a pNIPAM polymer brush with a thickness of 1.2 μm.

Controlled Growth of pNIPAM Brushes

The thickness of pNIPAM brushes can be controlled by varying the monomer concentration. Various monomer concentrations of NIPAM in DCM were subjected to the same polymerization conditions. The saturation limit of NIPAM in DCM was found to be 87% w/w. Different concentrations of NIPAM monomer were used ranging from 50 to 85% w/w (Table1) for polymerization at a fixed time of 24 hours.

Table 1. Surface selective pNIPAM brush thickness at different concentrations of monomer (pNIPAM) in DCM grown after 24 hours of UV λ = 350nm irradiation

wt% (*N*-isopropylacrylamide)	Thickness (nm)	Error ± (nm)
50	0	0
65	107	6
70	185	12
75	270	30
80	635	45
85	915	150

Brush thickness relative to monomer concentration is demonstrated in Figure 10. Concentrations below 50% w/w resulted in no polymer growth from the surface or in solution. The polymerization reaction from the surface in our case was limited by the amount of initiator and mass transport of monomer to the initiator. AIBN is a stable thermal initiator with a half-life on the order of hours.

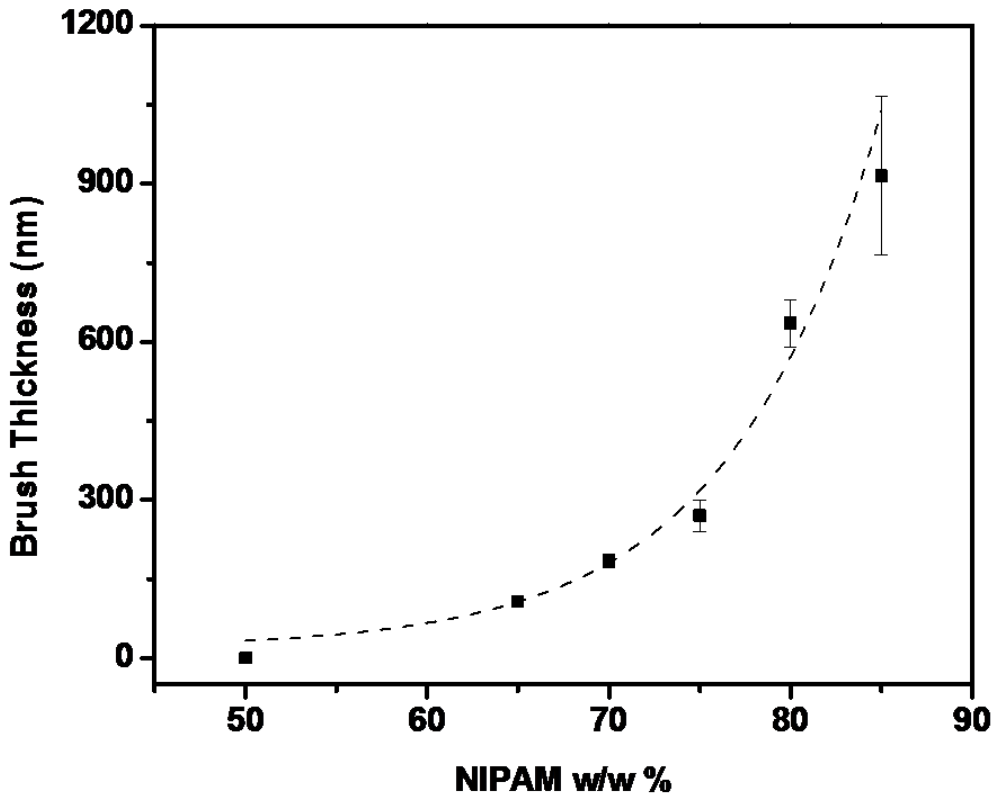

Figure 10. Thermo-responsive pNIPAM brushes on TiO_2 surfaces grown at different initial NIPAM monomer concentrations, % (w/w) in DCM solvent and UV (350nm) irradiated polymerized for 24 hours. Dashed line (--) is to guide the eye.

The longer the half-life, the longer the radical persists which increases the time frame in which a single initiator can start a polymerization once in contact with a monomer unit. In our case, the mobility of the monomer is limited by the diffusion rate through the solution. With low initiator concentrations and slow diffusion, the rate of initiation is minimal at lower monomer concentrations. At higher weight fractions, we were able to grow pNIPAM brushes a various thicknesses depending on the concentration of monomer (Figure 10). Brush thickness is reproducible for each weight fraction indicating a reproducible non-linear relationship between thickness and monomer concentration. The thickest brush of 1.2 μm was achieved at the saturation limit of NIPAM in DCM.

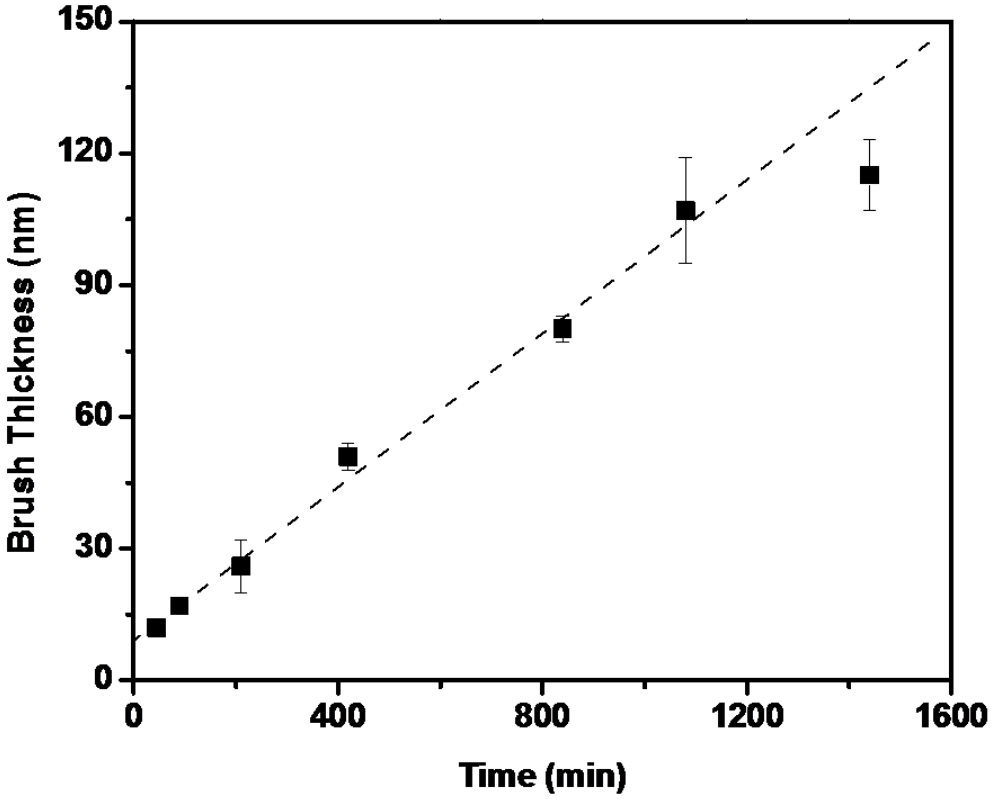

Figure 11. Polymerization time and brush thickness exhibiting a linear relationship with 65% w/w monomer in DCM. Dashed line (--) is to guide the eye.

Brush thickness was also characterized with respect to time at a constant NIPAM concentration of 65% w/w (Figure 11). A linear relationship in polymerization time and brush thickness was observed. The linear relation of photoinitiated polymerization with time proved the continuous generation of radicals which can diffuse through the already grown brush on the surfaces to react with more NIPAM monomer (Table 2).

Table 2. Relationship between dry pNIPAM brush thickness and UV irradiation time at 65% (w/w) *N*-isopropylacrylamide in DCM

Time (min)	Thickness (nm)	Error ±(nm)
45	12	2
90	17	2
210	26	6
420	51	3
840	80	3
1080	107	12
1440	115	8

After 20 hours, the polymerization ceased due the decay of UV generated radicals and reduction of diffusion of radicals through polymer brush.

Thermally Responsive Behavior of pNIPAM Brushes

Contact angle measurement

Static water contact angle measurements were used to investigate the surface wettabilities before and after the formation of orthogonal monolayers and pNIPAM brushes. The contact angle measurements were taken at room temperature and surfaces were N_2 dried before measurement.

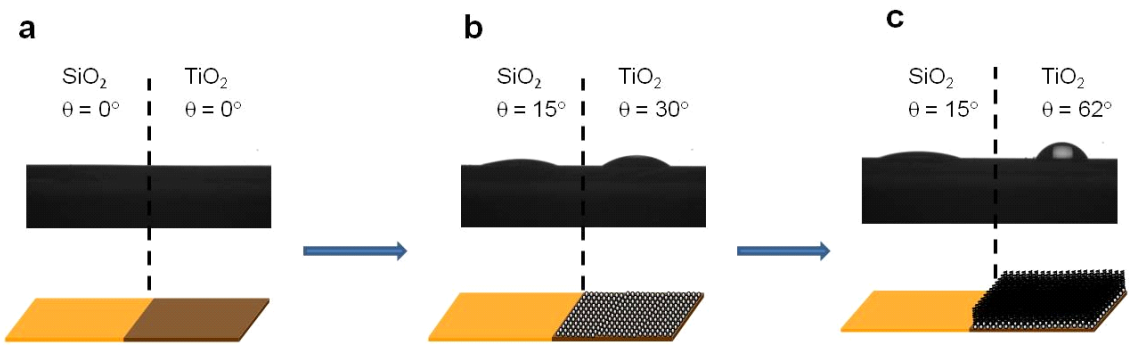

Figure 12. Static water contact angle on SiO_2-TiO_2 surfaces a) Bare surface, b) Orthogonal monolayer grown surface and c) Orthogonal pNIPAM brush grown surface. Contact angles on SiO_2-TiO_2 surfaces were measured after ringing with water and drying by purging N_2.

Figure 12 demonstrates the static contact angle changes due to formation of orthogonal monolayers and pNIPAM brushes on SiO_2-TiO_2 surfaces. Plasma clean SiO_2-TiO_2 patterned surface shows no contact angle on either oxide surface (Figure 12a) but once orthogonal self-assembled monolayer formed, the contact angle on TiO_2 surface was 30° and 15° on SiO_2 (Figure 12b). Contact angle on the pNIPAM brushes on TiO_2 surface was observed as 62 (Figure 12c) but on the on SiO_2 part of the surface the contact angle remain same as 15 which confirmed the surface selective growth of pNIPAM brushes (70-72).

To understand the surface wettability of the pNIPAM brushes above and below the LCST (32°C), we measured the contact angles at two different temperatures 40°C and 25°C (Figure 13). After soaking the film at 25°C for 20 min and then N_2 drying, a value of 62 was obtained indicating a hydrophilic surface. When immersing the substrate into water with temperatures above the LCST (40°C) for 20 min, the contact angle increased to 73°, which indicates the partial hydrophobic behavior of the pNIPAM brushes. At temperature below LCST, pNIPAM chains stay in an extended conformation due to the hydrogen bonding with water and amide group but above LCST, the pNIPAM brushes adopt a more collapsed confirmation due to the breaking of the hydrogen bonds with amide group which made pNIPAM brush more hydrophobic (75).

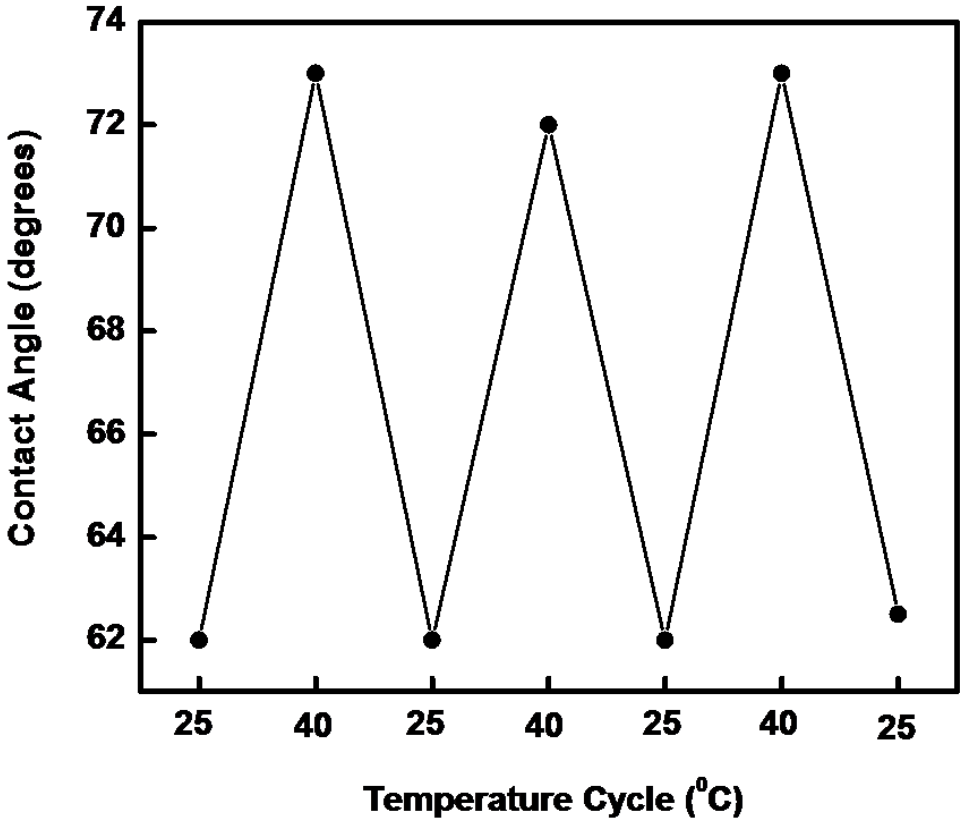

Figure 13. Transformation of static water contact angles on pNIPAM brushes on SiO_2-TiO_2 surfaces due to temperature cycling below (25°C) and above (40°C) LSCT. Contact angles were measured on the N_2 dried brush after soaking in water for 20 minute at 25°C and 40°C consecutively.

We also investigated the reversible thermo-responsive behavior of pNIPAM brushes. Figure 13 shows the contact angle on NIPAM polymer brush changes from 62 to 73 in below (25°C) and above (40°C) LSCT which was consistent in several temperature cycles.

Swelling Behavior of Orthogonal pNIPAM Brush

Dynamic tracking of pNIPAM swelling was monitored by spectroscopic ellipsometry. Several pNIPAM brushes were grown on a 3 cm by 1.5 cm substrates. Each layer was characterized by spectroscopic ellipsometry using *ex situ* measurements of Δ and Ψ and known refractive indices for the silicon, silicon oxide, and titanium oxide layers. The polymer film was characterized by fitting the brush thickness, refractive index, and extinction coefficient. The Cauchy model, Eq. 1, was used to fit the refractive index, n, while the Urbach equation, Eq. 2, was used to determine the extinction coefficient, k,

$$n = A + \frac{B}{l^2} + \frac{C}{l^4} \quad (1)$$

$$k = k_0 e^{D(E - B')} \quad (2)$$

where A, B, and C are Cauchy parameters and k_0 and D are Urhach parameters. Fitting the above model to the Δ and Ψ spectra produced an average refractive index of 1.52 ± 0.03 and extinction coefficient of 0.04 ± 0.005 at a wavelength of 632.8 nm. Most organic film models assume a value of zero for the extinction coefficient indicating no light scattering within the film. For thin NIPAM films, 20-30 nm, fitting the extinction coefficient results in a zero value. Thicker films exhibit non-zero values, which can be attributed to light scattering due to the heterogeneous nature of the film.

In situ tracking of the hydrogel swelling and collapse was performed at an angle of incidence of 60° in a custom flow cell. The substrate was immersed in 18 MΩ H_2O at 25°C for 1 hr to ensure that the polymer brush was intercalated with water. Spectral curves of Δ and Ψ were taken for several minutes prior to flowing in 50°C water followed by a rinse with 25°C water. Flowing in water above the LCST produces a change in Δ and Ψ due to polymer collapse, as shown in figure 14. In tracking mode the spectroscopic ellipsometer takes complete spectral data at each time interval.

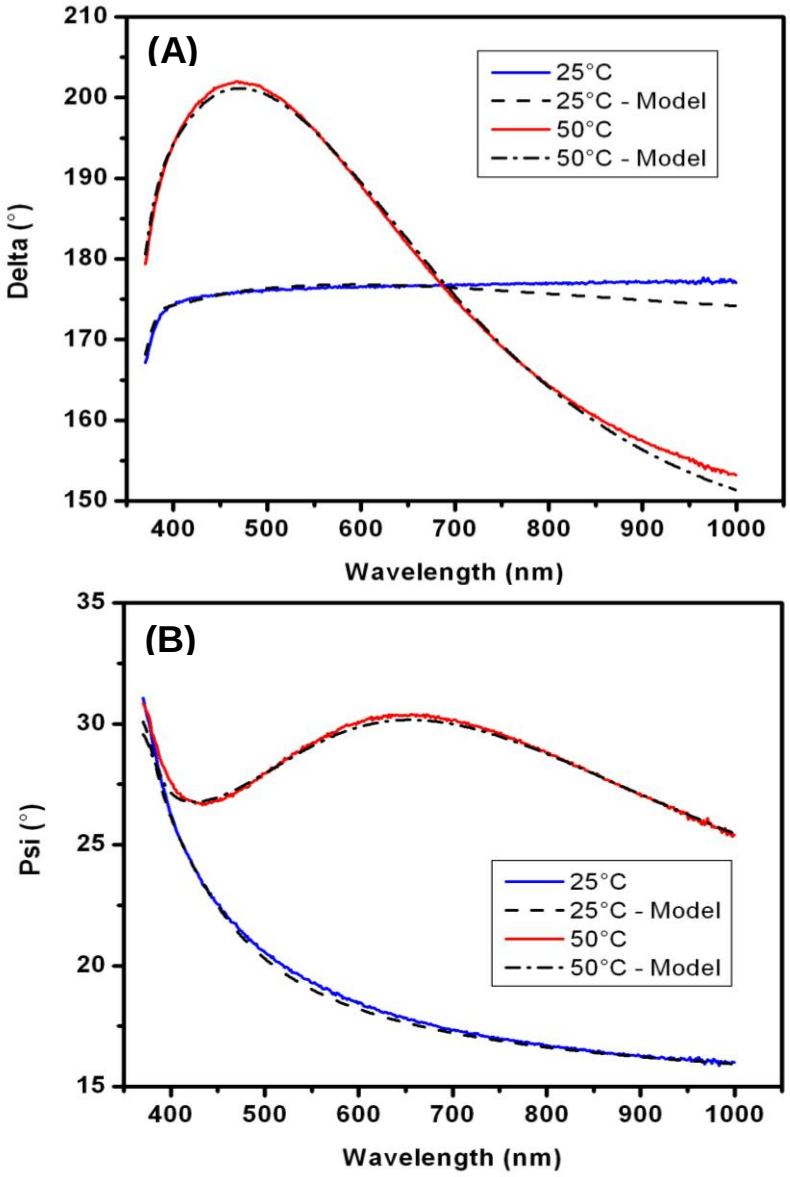

Figure 14. Spectropscopic ellipsometry values of delta and psi for NIPAM collapse due to temperature changes. Values are taken from an *in situ* experiment where a NIPAM film is cycled through collapse and swelling by changing solvent temperature from 25°C and 50°C, taken at 0min and 70 min, respectively. Dashed lines represent modeled values of delta and psi from fitted parameters; film thickness, refractive index, and extinction coefficient.

The dynamic data was modeled using equations 1 and 2. Changing the Cauchy and Urbach parameters produces the fits shown in figure 14 for the swollen and collapsed film. The modeled values for thickness, refractive index, and extinction coefficient for each time interval are reported in Figure 15. Injecting water above the LCST produces an immediate response in the polymer as indicated by the drastic decrease in brush thickness from 90 nm to 72 nm at 2 min.

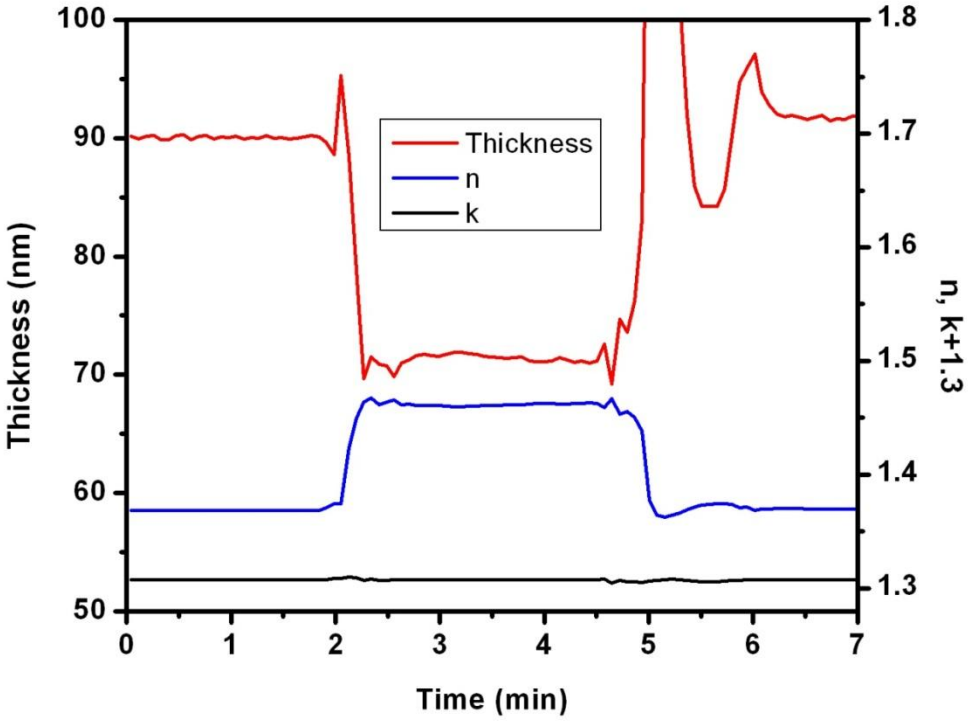

Figure 15. In situ spectroscopic elliposometry tracking NIPAM collapse due to solvent temperature changes. Thickness, refractive index, and extinction coefficients are derived from modeling delta and psi values. The film collapses when 50°C water is injected at

2min. Replacing the solvent with 25°C water swells the polymer to the starting thickness after a period of rearrangement.

Substantial changes in the film's refractive index are also observed. In the dry state the polymer brush has a refractive index of 1.52. The refractive index of the hydrogel resembles that of a polymer-water mixture producing an effective refractive index for the brush layer that is lower than the dry polymer. When the brush collapses, the polymer contracts squeezing water out of the film and the effective refractive index for the layer increases towards that of the dry film. Changes in the extinction coefficient are not observed indicating similar light scattering properties for the swollen and collapsed film. In figure 15, an adjustment factor of 1.3 was used to plot the extinction coefficient on the same scale as refractive index. The extinction coefficient during the dynamic tracking fluctuates within the range reported for the dry film.

Limiting the organic brush model to a single layer provides the effective refractive index for that layer. The layer is actually a mixture of water and polymer each with distinct refractive indices and volume fractions. By applying the Maxwell-Garnett effective medium approximation, Eq. 3,

$$\frac{n_{eff}^{\ 2} - n^2_{\ p}}{n_{eff}^{\ 2} + 2n^2_{\ p}} = \Phi_w \frac{n_w^{\ 2} - n^2_{\ p}}{n_w^{\ 2} + 2n^2_{\ p}} \qquad (3)$$

where n_p and n_w are the refractive indices for pNIPAM and water, n_{eff} is the modeled refractive index profile, and Φ_w is the water volume fraction within the hydrogel which was computed over the dynamic range, Figure 16. The refractive index of the dry polymer was used for n_p and a value of 1.33 was used for n_w. Below the LCST the hydrogel is swollen with a 0.80 water volume fraction. In the collapsed state, above the LCST, the polymer film contains a 0.30 water volume fraction within a smaller volume than the swollen state.

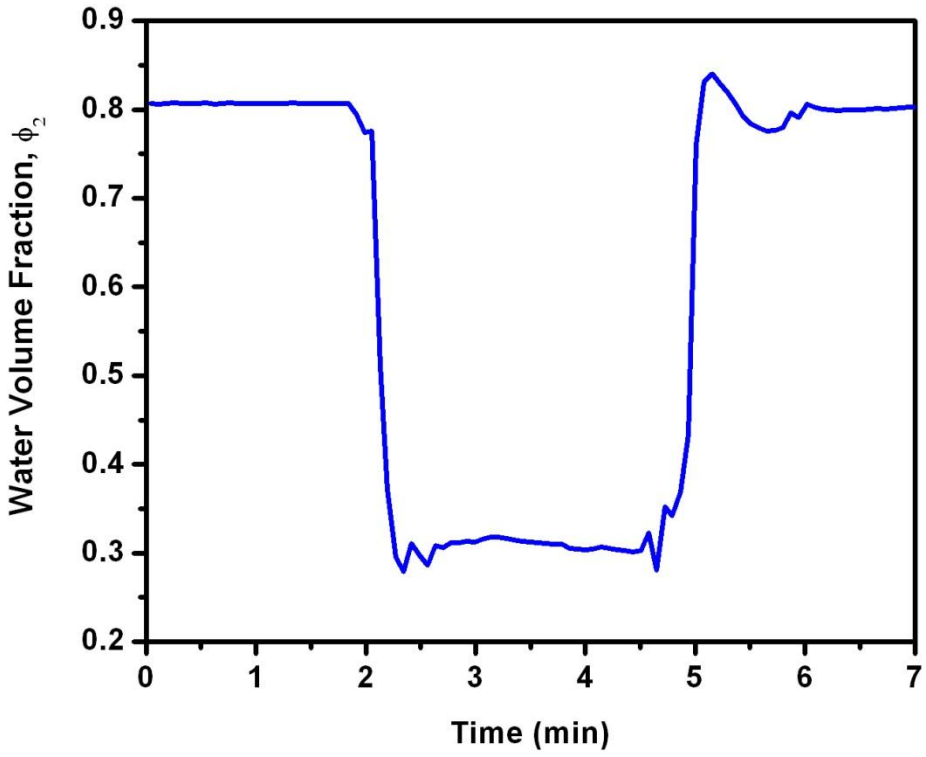

Figure 16. Volume fraction of water in the NIPAM brush as computed by the Maxwell-Garnett effective medium approximation. The dynamic data starts out with a swollen brush at 25°C. Water is released when the film contracts reducing the volume fraction in the thinner collapsed film.

In raising the temperature above the LCST, the hydrogel loses ~70% of water from the swollen volume due to polymer contraction. Using a temperature of 50°C the polymer contracts completely within 25 seconds. Injecting 25°C water at 4.5 min the polymer is taken below the LCST and the film again swells to a 0.80 water volume fraction in ~30 sec. Re-swelling of the pNIPAM involves rearrangement of the polymer brush which is expected to take longer than polymer contraction. For each case, collapse or re-swelling, changes in the film occur rapidly at the experimental temperatures. Fluctuations in the dynamic data after the initial swelling also indicate some rearrangement within the film, as is evident in Figure 15 and 16.

CHAPTER 5

CONCLUSION

This research work has been performed in three logical steps involving the 1. Synthesis of photo initiator for orthogonal self assembly on multi component surfaces, 2. Homogeneous grafting of thermo-responsive polymer brush on the selective surfaces and 3. Characterization of thermo-responsive behavior of grafted polymer brushes. Initially we have synthesized catechol based photo-initiator and used this initiator to orthogonally self-assemble onto the TiO_2 side of SiO_2-TiO_2 dual surfaces. After successful initiator immobilization, we grafted thermo-responsive pNIPAM brush on the monolayer using UV irradiation, which yielded densely packed polymer layers selectively on TiO_2. Selective growth of thick and homogeneous pNIPAM brush was confirmed using FTIR and SEM.

The growth of the polymer brush layer was controlled by changing concentration of monomer in the solvent and polymerization time. The grown pNIPAM brush was found to have thermo-responsive behavior gaining hydrophobic characteristics above its LCST. Also this thermo-responsive behavior was found be reversible with many cycles. Our swelling study showed the volumetric change below and above LCST due to gain and release of water from polymer brushes.

The result of this research is significant from several points of view. First of all, the surface selective growth of polymer brushes opens the door for nanoscale surface patterning. Secondly, the possibility of targeting functionality on multi-component surfaces is of great utility on irregularly shaped objects or nanoscale systems. Thirdly, the growth of thick and homogenous growth of thermo-responsive polymer brushes are now available to investigate different biomedical applications such as drug delivery. Overall, this research work is a successful representation of the surface selective growth of stimuli-responsive brushes on multi-component surfaces.

REFERENCES

1. Brittain, W. J.; Minko, S., A structural definition of polymer brushes. Journal of Polymer Science Part A: Polymer Chemistry **2007,** 45 (16), 3505-3512.

2. MILNER, S. T., Polymer Brushes. Science **1991,** 251 (4996), 905-914.

3. Orski, S. V.; Fries, K. H.; Sontag, S. K.; Locklin, J., Fabrication of nanostructures using polymer brushes. Journal of Materials Chemistry **2011**.

4. Kent, M. S., A quantitative study of tethered chains in various solution conditions using Langmuir diblock copolymer monolayers. Macromolecular Rapid Communications **2000,** 21 (6), 243-270.

5. Cosgrove, T.; Heath, T. G.; Ryan, K.; Crowley, T. L., Neutron scattering from adsorbed polymer layers. Macromolecules **1987,** 20 (11), 2879-2882.

6. Parsonage, E.; Tirrell, M.; Watanabe, H.; Nuzzo, R. G., Adsorption of poly(2-vinylpyridine)-poly (styrene) block copolymers from toluene solutions. Macromolecules **1991,** 24 (8), 1987-1995.

7. Mansky, P.; Liu, Y.; Huang, E.; Russell, T. P.; Hawker, C., Controlling Polymer-Surface Interactions with Random Copolymer Brushes. Science **1997,** 275 (5305), 1458-1460.

8. Zhao, B.; Brittain, W. J., Polymer brushes: surface-immobilized macromolecules. Progress in Polymer Science **2000,** 25 (5), 677-710.

9. Jones, D. M.; Brown, A. A.; Huck, W. T. S., Surface-Initiated Polymerizations in Aqueous Media: Effect of Initiator Density. Langmuir **2002,** 18 (4), 1265-1269.

10. Wu, T.; Efimenko, K.; Genzer, J., Combinatorial Study of the Mushroom-to-Brush Crossover in Surface Anchored Polyacrylamide. Journal of the American Chemical Society **2002,** 124 (32), 9394-9395.

11. Prucker, O.; Rühe, J., Synthesis of Poly(styrene) Monolayers Attached to High Surface Area Silica Gels through Self-Assembled Monolayers of Azo Initiators. Macromolecules **1998,** 31 (3), 592-601.

12. Advincula, R. C. ; Brittain, W. J. ; Caster, K. C.; Ruhe, J., *Polymer Brushes: Synthesis,Characterization, Applications* (John Wiley & Sons, New York, 2004).

13. Prucker, O.; Rühe, J., Mechanism of Radical Chain Polymerizations Initiated by Azo Compounds Covalently Bound to the Surface of Spherical Particles. *Macromolecules* **1998,** *31* (3), 602-613.

14. Kaholek, M.; Lee, W.-K.; Feng, J.; LaMattina, B.; Dyer, D. J.; Zauscher, S., Weak Polyelectrolyte Brush Arrays Fabricated by Combining Electron-Beam Lithography with Surface-Initiated Photopolymerization. *Chemistry of Materials* **2006,** *18* (16), 3660-3664.

15. Beinhoff, M.; Frommer, J.; Carter, K. R., Photochemical Attachment of Reactive Cross-Linked Polymer Films to Si/SiO2 Surfaces and Subsequent Polymer Brush Growth. *Chemistry of Materials* **2006,** *18* (15), 3425-3431.

16. Paul, R.; Schmidt, R.; Feng, J.; Dyer, D. J., Photoinitiated polymerization of styrene from self-assembled monolayers on gold. II. Grafting rates and extraction. *Journal of Polymer Science Part A: Polymer Chemistry* **2002,** *40* (19), 3284-3291.

17. Ionov, L.; Minko, S.; Stamm, M.; Gohy, J.-F.; Jérôme, R.; Scholl, A., Reversible Chemical Patterning on Stimuli-Responsive Polymer Film: Environment-Responsive Lithography. *Journal of the American Chemical Society* **2003,** *125* (27), 8302-8306.

18. Ulbricht, M.; Yang, H., Porous Polypropylene Membranes with Different Carboxyl Polymer Brush Layers for Reversible Protein Binding via Surface-Initiated Graft Copolymerization. *Chemistry of Materials* **2005,** *17* (10), 2622-2631.

19. Luzinov, I.; Tsukruk, V. V., Ultrathin Triblock Copolymer Films on Tailored Polymer Brushes. *Macromolecules* **2002,** *35* (15), 5963-5973.

20. Long, J. R.; Oyler, N.; Drobny, G. P.; Stayton, P. S., Assembly of α-helical Peptide Coatings on Hydrophobic Surfaces. *Journal of the American Chemical Society* **2002,** *124* (22), 6297-6303.

21. Frey, W.; Meyer, D. E.; Chilkoti, A., Thermodynamically Reversible Addressing of a Stimuli Responsive Fusion Protein onto a Patterned Surface Template†. *Langmuir* **2003,** *19* (5), 1641-1653.

22. Klee, D.; Ademovic, Z.; Bosserhoff, A.; Hoecker, H.; Maziolis, G.; Erli, H.-J., Surface modification of poly(vinylidenefluoride) to improve the osteoblast adhesion. *Biomaterials* **2003,** *24* (21), 3663-3670.

23. Pale-Grosdemange, C.; Simon, E. S.; Prime, K. L.; Whitesides, G. M., Formation of self-assembled monolayers by chemisorption of derivatives of oligo(ethylene glycol) of structure HS(CH2)11(OCH2CH2)mOH on gold. *Journal of the American Chemical Society* **1991,** *113* (1), 12-20.

24. Herrwerth, S.; Eck, W.; Reinhardt, S.; Grunze, M., Factors that Determine the Protein Resistance of Oligoether Self-Assembled Monolayers − Internal Hydrophilicity, Terminal Hydrophilicity, and Lateral Packing Density. *Journal of the American Chemical Society* **2003,** *125* (31), 9359-9366.

25. Kingshott, P.; Wei, J.; Bagge-Ravn, D.; Gadegaard, N.; Gram, L., Covalent Attachment of Poly(ethylene glycol) to Surfaces, Critical for Reducing Bacterial Adhesion. *Langmuir* **2003,** *19* (17), 6912-6921.

26. Zheng, M.; Davidson, F.; Huang, X., Ethylene Glycol Monolayer Protected Nanoparticles for Eliminating Nonspecific Binding with Biological Molecules†. *Journal of the American Chemical Society* **2003,** *125* (26), 7790-7791.

27. de Gennes, P.-G., Ultradivided matter. *Nature* **2001,** *412* (6845), 385-385.

28. Gay, C., Wetting of a Polymer Brush by a Chemically Identical Polymer Melt. *Macromolecules* **1997,** *30* (19), 5939-5943.

29. Kawai, T.; Saito, K.; Lee, W., Protein binding to polymer brush, based on ion-exchange, hydrophobic, and affinity interactions. *Journal of Chromatography B* **2003,** *790* (1-2), 131-142.

30. van Zanten, J. H., Terminally Anchored Chain Interphases: Their Chromatographic Properties. *Macromolecules* **1994,** *27* (23), 6797-6807.

31. Israels, R.; Gersappe, D.; Fasolka, M.; Roberts, V. A.; Balazs, A. C., pH-Controlled Gating in Polymer Brushes. *Macromolecules* **1994,** *27* (22), 6679-6682.

32. Sevick, E. M.; Williams, D. R. M., Polymer Brushes as Pressure-Sensitive Automated Microvalves. *Macromolecules* **1994,** *27* (19), 5285-5290.

33. Israels, R.; Gersappe, D.; Fasolka, M.; Roberts, V. A.; Balazs, A. C., pH-Controlled Gating in Polymer Brushes. *Macromolecules* **1994,** *27* (22), 6679-6682.

34. von Werne, T. A.; Germack, D. S.; Hagberg, E. C.; Sheares, V. V.; Hawker, C. J.; Carter, K. R., A Versatile Method for Tuning the Chemistry and Size of Nanoscopic Features by Living Free Radical Polymerization. *Journal of the American Chemical Society* **2003,** *125* (13), 3831-3838.

35. von Werne, T. A.; Germack, D. S.; Hagberg, E. C.; Sheares, V. V.; Hawker, C. J.; Carter, K. R., A Versatile Method for Tuning the Chemistry and Size of Nanoscopic Features by Living Free Radical Polymerization. *Journal of the American Chemical Society* **2003,** *125* (13), 3831-3838.

36. Zhou, F.; Liu, W.; Hao, J.; Xu, T.; Chen, M.; Xue, Q., Fabrication of Conducting Polymer and Complementary Gold Microstructures Using Polymer Brushes as Templates. *Advanced Functional Materials* **2003,** *13* (12), 938-942.

37. Juang, A.; Scherman, O. A.; Grubbs, R. H.; Lewis, N. S., Formation of Covalently Attached Polymer Overlayers on Si(111) Surfaces Using Ring-Opening Metathesis Polymerization Methods. *Langmuir* **2001,** *17* (5), 1321-1323.

38. Bergbreiter, D. E.; Liu, M. L., Polythiophene formation within hyperbranched grafts on polyethylene films. *Journal of Polymer Science Part A: Polymer Chemistry* **2001,** *39* (23), 4119-4128.

39. Moon, J. H.; Swager, T. M., Poly(p-phenylene ethynylene) Brushes. *Macromolecules* **2002,** *35* (16), 6086-6089.

40. Ionov, L.; Sapra, S.; Synytska, A.; Rogach, A. L.; Stamm, M.; Diez, S., Fast and Spatially Resolved Environmental Probing Using Stimuli-Responsive Polymer Layers and Fluorescent Nanocrystals. *Advanced Materials* **2006,** *18* (11), 1453-1457.

41. Kumar, A.; Srivastava, A.; Galaev, I. Y.; Mattiasson, B., Smart polymers: Physical forms and bioengineering applications. *Progress in Polymer Science* **2007,** *32* (10), 1205-1237.

42. Ulbricht, M., Advanced functional polymer membranes. *Polymer* **2006,** *47* (7), 2217-2262.

43. Stuart, M. A. C.; Huck, W. T. S.; Genzer, J.; Muller, M.; Ober, C.; Stamm, M.; Sukhorukov, G. B.; Szleifer, I.; Tsukruk, V. V.; Urban, M.; Winnik, F.; Zauscher, S.; Luzinov, I.; Minko, S., Emerging applications of stimuli-responsive polymer materials. *Nat Mater* **2010,** *9* (2), 101-113.

44. Y.G. Takei, T. Aoki, K. Sanui, N. Ogata, Y. Sakurai, T. Okano, Macromolecules 1994, 27, 6163–6166.

45. Rzaev, Z. M. O.; Dinçer, S.; Piskin, E., Functional copolymers of N-isopropylacrylamide for bioengineering applications. *Progress in Polymer Science* **2007,** *32* (5), 534-595.

46. de Jong, J.; Lammertink, R. G. H.; Wessling, M., Membranes and microfluidics: a review. *Lab on a Chip* **2006,** *6* (9), 1125-1139.

47. Eddington, D. T.; Beebe, D. J., Flow control with hydrogels. *Advanced Drug Delivery Reviews* **2004,** *56* (2), 199-210.

48. Beebe, D. J.; Moore, J. S.; Bauer, J. M.; Yu, Q.; Liu, R. H.; Devadoss, C.; Jo, B.-H., Functional hydrogel structures for autonomous flow control inside microfluidic channels. *Nature* **2000,** *404* (6778), 588-590.

49. Geismann, C.; Yaroshchuk, A.; Ulbricht, M., Permeability and Electrokinetic Characterization of Poly(ethylene terephthalate) Capillary Pore Membranes with Grafted Temperature-Responsive Polymers†. *Langmuir* **2006,** *23* (1), 76-83.

50. Friebe, A.; Ulbricht, M., Controlled Pore Functionalization of Poly(ethylene terephthalate) Track-Etched Membranes via Surface-Initiated Atom Transfer Radical Polymerization. *Langmuir* **2007,** *23* (20), 10316-10322.

51. Friebe, A.; Ulbricht, M., Cylindrical Pores Responding to Two Different Stimuli via Surface-Initiated Atom Transfer Radical Polymerization for Synthesis of Grafted Diblock Copolymers. *Macromolecules* **2009,** *42* (6), 1838-1848.

52. Wu, C.; Wang, X., Globule-to-Coil Transition of a Single Homopolymer Chain in Solution. *Physical Review Letters* **1998,** *80* (18), 4092.

53. Yan, H.; Tsujii, K., Potential application of poly(N-isopropylacrylamide) gel containing polymeric micelles to drug delivery systems. *Colloids and Surfaces B: Biointerfaces* **2005,** *46* (3), 142-146.

54. LAIBINIS, P. E.; HICKMAN, J. J.; WRIGHTON, M. S.; WHITESIDES, G. M., Orthogonal Self-Assembled Monolayers: Alkanethiols on Gold and Alkane Carboxylic Acids on Alumina. *Science* **1989,** *245* (4920), 845-847.

55. Hickman, J. J.; Laibinis, P. E.; Auerbach, D. I.; Zou, C.; Gardner, T. J.; Whitesides, G. M.; Wrighton, M. S., Toward orthogonal self-assembly of redox active molecules on platinum and gold: selective reaction of disulfide with gold and isocyanide with platinum. *Langmuir* **1992,** *8* (2), 357-359.

56. Martin, B. R.; Dermody, D. J.; Reiss, B. D.; Fang, M.; Lyon, L. A.; Natan, M. J.; Mallouk, T. E., Orthogonal Self-Assembly on Colloidal Gold-Platinum Nanorods. *Advanced Materials* **1999,** *11* (12), 1021-1025.

57. del Campo, A.; Boos, D.; Spiess, H. W.; Jonas, U., Surface Modification with Orthogonal Photosensitive Silanes for Sequential Chemical Lithography and Site-Selective Particle Deposition. *Angewandte Chemie International Edition* **2005,** *44* (30), 4707-4712.

58. Ulman, A., Formation and Structure of Self-Assembled Monolayers. *Chemical Reviews* **1996,** *96* (4), 1533-1554.

579 Frei, H.; Fitzmaurice, D. J.; Graetzel, M., Surface chelation of semiconductors and interfacial electron transfer. *Langmuir* **1990,** *6* (1), 198-206.

60. Martin, S. T.; Kesselman, J. M.; Park, D. S.; Lewis, N. S.; Hoffmann, M. R., Surface Structures of 4-Chlorocatechol Adsorbed on Titanium Dioxide. *Environmental Science & Technology* **1996,** *30* (8), 2535-2542.

61. Vasudevan, D.; Stone, A. T., Adsorption of Catechols, 2-Aminophenols, and 1,2-Phenylenediamines at the Metal (Hydr)Oxide/Water Interface: Effect of Ring Substituents on the Adsorption onto TiO2. *Environmental Science & Technology* **1996,** *30* (5), 1604-1613.

62. Moser, J.; Punchihewa, S.; Infelta, P. P.; Graetzel, M., Surface complexation of colloidal semiconductors strongly enhances interfacial electron-transfer rates. *Langmuir* **1991,** *7* (12), 3012-3018.

63. Connor, P. A.; Dobson, K. D.; McQuillan, A. J., New Sol-Gel Attenuated Total Reflection Infrared Spectroscopic Method for Analysis of Adsorption at Metal Oxide Surfaces in Aqueous Solutions. Chelation of TiO2, ZrO2, and Al2O3 Surfaces by Catechol, 8-Quinolinol, and Acetylacetone. *Langmuir* **1995,** *11* (11), 4193-4195.

64. Tulevski, G. S.; Miao, Q.; Fukuto, M.; Abram, R.; Ocko, B.; Pindak, R.; Steigerwald, M. L.; Kagan, C. R.; Nuckolls, C., Attaching Organic Semiconductors to Gate Oxides: In Situ Assembly of Monolayer Field Effect Transistors. *Journal of the American Chemical Society* **2004,** *126* (46), 15048-15050.

65. Fan, X.; Lin, L.; Dalsin, J. L.; Messersmith, P. B., Biomimetic Anchor for Surface-Initiated Polymerization from Metal Substrates. *Journal of the American Chemical Society* **2005,** *127* (45), 15843-15847.

66. Dalsin, J. L.; Lin, L.; Tosatti, S.; Vörös, J.; Textor, M.; Messersmith, P. B., Protein Resistance of Titanium Oxide Surfaces Modified by Biologically Inspired mPEG−DOPA. *Langmuir* **2004,** *21* (2), 640-646.

67. Malisova, B.; Tosatti, S.; Textor, M.; Gademann, K.; Zürcher, S., Poly(ethylene glycol) Adlayers Immobilized to Metal Oxide Substrates Through Catechol Derivatives: Influence of Assembly Conditions on Formation and Stability. *Langmuir* **2010,** *26* (6), 4018-4026.

68. Wang, S.; Zhu, Y., Facile Method to Prepare Smooth and Homogeneous Polymer Brush Surfaces of Varied Brush Thickness and Grafting Density. Langmuir **2009,** 25 (23), 13448-13455.

69. Tu, H.; Heitzman, C. E.; Braun, P. V., Patterned Poly(N-isopropylacrylamide) Brushes on Silica Surfaces by Microcontact Printing Followed by Surface-Initiated Polymerization. Langmuir **2004,** 20 (19), 8313-8320.

70. He, Q.; Küller, A.; Grunze, M.; Li, J., Fabrication of Thermosensitive Polymer Nanopatterns through Chemical Lithography and Atom Transfer Radical Polymerization. Langmuir **2007,** 23 (7), 3981-3987.

71. Estillore, N. C.; Park, J. Y.; Advincula, R. C., Langmuir−Schaefer (LS) Macroinitiator Film Control on the Grafting of a Thermosensitive Polymer Brush via Surface Initiated-ATRP. Macromolecules **2010,** 43 (16), 6588-6598.

72. Jia, X.; Jiang, X.; Liu, R.; Yin, J., Poly(N-isopropylacrylamide) Brush Fabricated by Surface-Initiated Photopolymerization and its Response to Temperature. Macromolecular Chemistry and Physics **2009,** 210 (21), 1876-1882.

73. Yim, H.; Kent, M. S.; Mendez, S.; Balamurugan, S. S.; Balamurugan, S.; Lopez, G. P.; Satija, S., Temperature-Dependent Conformational Change of PNIPAM Grafted Chains at High Surface Density in Water. Macromolecules **2004,** 37 (5), 1994-1997.

74. Plunkett, K. N.; Zhu, X.; Moore, J. S.; Leckband, D. E., PNIPAM Chain Collapse Depends on the Molecular Weight and Grafting Density. Langmuir **2006,** 22 (9), 4259-4266.

75. Annaka, M.; Yahiro, C.; Nagase, K.; Kikuchi, A.; Okano, T., Real-time observation of coil-to-globule transition in thermosensitive poly(N-isopropylacrylamide) brushes by quartz crystal microbalance. Polymer **2007,** 48 (19), 5713-5720.